BIOCHEMISTRY
including biophysical chemistry & molecular biology

Article

pubs.acs.org/biochemistry

Differences in the Structural Stability and Cooperativity between Monomeric Variants of Natural and de Novo Cro Proteins Revealed by High-Pressure Fourier Transform Infrared Spectroscopy

Hiroshi Imamura,[†] Yasuhiro Isogai,[‡] and Minoru Kato*[,†,§]

[†]Department of Pharmacy, College of Pharmaceutical Sciences, Ritsumeikan University, 1-1-1 Nojihigashi, Kusatsu, Shiga 525-8577, Japan

[‡]Department of Biotechnology, Faculty of Engineering, Toyama Prefectural University, Imizu, Toyama 939-0398, Japan

[§]Graduate School of Science and Engineering, Ritsumeikan University, 1-1-1 Nojihigashi, Kusatsu, Shiga 525-8577, Japan

Supporting Information

ABSTRACT: It is widely accepted that pressure affects the structure and dynamics of proteins; however, the underlying mechanism remains unresolved. Our previous studies have investigated the effects of pressure on fundamental secondary structural elements using model peptides, because these peptides represent a basis for understanding the effects of pressure on more complex structures. This study targeted monomeric variants of naturally occurring bacteriophage λ Cro (natural Cro) and de novo designed λ Cro (SN4m), which are α + β proteins. The sequence of SN4m is 75% different from that of natural Cro, but the structures are almost identical. Consequently, a comparison of the folding properties of these proteins is of interest. Pressure- and temperature-variable Fourier transform infrared spectroscopic analyses revealed that the α-helices and β-sheets of natural Cro are cooperatively and reversibly unfolded by pressure and temperature, whereas those of SN4m are not cooperatively unfolded by pressure; i.e., the α-helices of SN4m unfold at significantly higher pressures than the β-sheets and irreversibly unfold with increases in temperature. The higher unfolding pressure for the α-helices of SN4m indicates the presence of an intermediate structure of SN4m that does not retain β-sheet structure but does preserve the α-helices. These results demonstrate that the α-helices of natural Cro are stabilized by global tertiary contacts among the α-helices and the β-sheets, whereas the α-helices of SN4m are stabilized by local tertiary contacts between the α-helices.

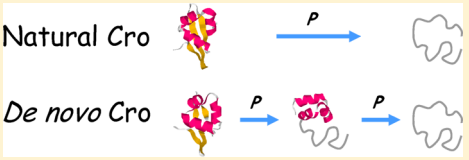

Conformational changes in proteins can be induced by varying temperature and pressure. Investigating the effects of temperature and pressure on protein structures is fundamentally important for understanding protein folding. However, the molecular basis of the effects of pressure on protein folding (denaturation) remains unresolved compared with our molecular understanding of heat-induced denaturation. It has been suggested that unfolding of a protein with pressure significantly depends on changes in the void volume and hydration surrounding a protein molecule.[1−4] The establishment of a clear molecular understanding of protein unfolding because of pressure will be helpful in developing a comprehensive picture of protein folding. The complex nature of a protein system makes it difficult for experimental and theoretical studies to demonstrate the microscopic behavior of protein denaturation. Thus, systematic research based on the hierarchical aspect of protein structure represents an effective approach for reaching a comprehensive understanding of pressure denaturation of proteins. Recently, we have focused on the effects of pressure on secondary structures of model peptides.[5−8] These works provided an interesting common phenomenon: all the α-helices we examined are folded by pressure, and this contrasts the pressure-induced unfolding of protein's helices.[9,10] In the previous reports,[7,8] we proposed that the helices of proteins are inherently stabilized by pressure but unfold if their surrounding hydrophobic environment is disrupted by pressure, because hydrated helices are quite unstable. Conversely, for β-sheet structures, we observed that a β-hairpin peptide composed of two β-sheets with a turn is unfolded by pressure (H. Imamura and M. Kato, manuscript in preparation). The pressure-dependent behavior of these fundamental secondary structure elements provides a basis for interpreting the effects of pressure on more complex structures in proteins.

This study targets the α + β protein, bacteriophage λ Cro, a naturally occurring DNA-binding protein, in which the α-helices and β-sheets are in contact with each other and share the hydrophobic core.[11] This hydrophobic core most likely contributes to the structural stability and cooperative character observed in the folding−unfolding process of this protein. In general, the amide I peaks due to α-helices and β-sheets are separately observed in the FTIR spectrum. Thus, conformational changes of the α-helices and β-sheets can be simultaneously monitored by FTIR spectroscopy. This allows us to examine the cooperative behavior of the protein. As mentioned above, an increase in pressure induces helical

Received: December 26, 2011
Revised: April 3, 2012
Published: April 6, 2012

   dx.doi.org/10.1021/bi2019223 | *Biochemistry* 2012, 51, 3539−3546

peptides to refold. Characterizing whether such anomalous behavior is observed in an $\alpha + \beta$ protein will be interesting.

The previous pressure studies targeting $\alpha + \beta$ proteins have employed naturally occurring proteins such as ribonuclease A,[10,12] lysozyme,[13] and ubiquitin.[14] In the study presented here, by employing λ Cro as the target protein, we can compare the structural stability of the native and artificial proteins. An artificial protein sequence forming the $\alpha + \beta$ structures similar to those of bacteriophage λ Cro has been successfully designed and produced using a computational method with empirical potential functions.[15] The sequence of the designed λ Cro is 75% different from that of native λ Cro.[11] The NMR structure of the designed λ Cro monomer (SN4m) in solution has been determined and found to be almost identical to the backbone structure of a monomeric variant of native λ Cro, which is termed natural Cro hereafter, as shown in Figure 1. For protein

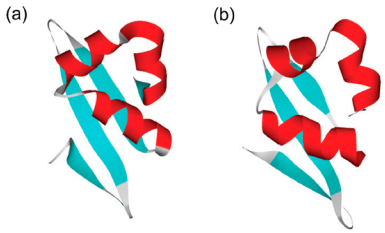

Figure 1. Structures of (a) natural Cro (monomeric λ Cro, PDB entry 1ORC) and (b) SN4m (designed monomeric λ Cro, PDB entry 2CW1). The root-mean-square deviation of the main chain atoms between SN4m and natural Cro is 2.1 Å.

design, it is important to compare the folding characteristics such as thermodynamic stability and folding cooperativity between the designed and natural proteins, because the folding characteristics of natural proteins can be related to their function. In this study, thus, we also investigated the folding properties of SN4m and compared the results with those obtained for natural Cro. In particular, the pressure perturbation comparison between the natural protein and a designed analogue represents the first study to employ pressure as a way of examining protein design characteristics. We show that the loose contacts between the α-helices and β-sheets in the hydrophobic core underlie loss of cooperativity in the pressure-induced unfolding of SN4m. These findings are important for the further design of de novo proteins and provide insights into the mechanisms of structural stability of naturally occurring proteins.

MATERIALS AND METHODS

Sample Preparation. The sequences of natural Cro and SN4m are ME***QRIT***LKDYAMRFGQTKTAKDLGVYQSAIN-KAIHAGRK***IFLTI***NADGSV***YAEEVK***DG***EVK***PFPS and MRKKLDLKKFVEDKNQEYAARALGLSQKLIEEVLKRGLP-VYV***ET***NKDGN***IK***V***YITQ***DG***ITQP***FPP, respectively. Here, the underline indicates the α-helix and the boldface italics the β-sheet structures, respectively, derived from the NMR solution structures (PDB entries 2ORC for natural Cro and 2CW1 for SN4m). Both proteins were expressed in *Escherichia coli* and purified as previously reported.[15] The proteins were dialyzed against an appropriate buffer solution and water to remove trifluoroacetic acid (TFA), which was used in the high-performance liquid chromatography purification step, and lyophilized. TFA shows a strong infrared absorbance at ~1673 cm^{-1} (from ref 16) that obscures the band at ~1676 cm^{-1} arising from an antiparallel β-sheet in an amide I′ band of a protein. The lyophilized proteins were dissolved in a 50 mM HEPES-NaOD/D_2O solution containing 100 mM NaCl and centrifuged to remove precipitates. The resulting solutions had a pD of 7.4. All samples were prepared at ~4 °C to prevent aggregation. The concentrations of natural Cro and SN4m were spectrophotometrically determined to be 1.8 and 1.4 mM, respectively, using an ε_{274} of 4260 M^{-1} cm^{-1}.[17]

FTIR Measurements. The sample was loaded into a cell with CaF_2 windows and a 30 μm polytetrafluoroethylene spacer for the temperature-variable measurements. For the pressure-variable measurements, a diamond anvil cell with gaskets with thicknesses of 50 μm (natural Cro) and 100 μm (SN4m) was used. Both cells were connected to a circulating water bath to control the sample temperature (±0.1 °C). IR spectra were recorded on a FTIR spectrometer (Jasco FT/IR-680 plus or a Jasco FT/IR-6100) equipped with a DLATGS detector for temperature-variable measurements or with a MCT liquid nitrogen-cooled detector for pressure-variable measurements. α-Quartz was added to the samples as an internal pressure calibrant.[18] Prior to each measurement, the protein solution was incubated at room temperature for ~1 h. The completion of hydrogen−deuterium exchange of the amide protons was confirmed by monitoring the intensity of the amide II band. Typically, 256 interferograms were collected to obtain a spectrum with a resolution of 2 cm^{-1}. Spectral analyses were performed using GRAMS Research for System2000 FTIR version 3.01B (Galactic Software).

Circular Dichroism Measurements. Circular dichroism (CD) spectra were recorded using a Jasco J-805 CD spectrometer equipped with a temperature-controlled cell with a 30 μm path length. The cell was connected to a circulating water bath to control the sample temperature (±0.1 °C). The protein concentration and the solvent used for the CD measurement of natural Cro and SN4m are the same as those used for the FTIR measurements. To examine the temperature dependence of the mean residue ellipticities at 222 nm for natural Cro, the sample was heated at a heating rate of 2 °C/min. The raw ellipticity values were converted to the mean residue ellipticity values using the equation $[\theta] = \theta_{obs}/(10ncl)$, where θ_{obs} is the observed ellipticity, l is the optical path length (centimeters), c is the concentration of the peptide (molar), and n is the number of residues.

Thermodynamic Analysis. To examine the thermodynamic characteristics of denaturation using the CD or FTIR data, we assumed the two-state model: the equilibrium K constant between the folded (F) and unfolded (U) states was obtained from the equation

$$K = [U]/[F] = (1 - f)/f \quad [f = [F]/([F] + [U])] \qquad (1)$$

The values of f were determined according to the following equation:

$$f = \frac{I_U - I}{I_U - I_F} \qquad (2)$$

where I_F and I_U are the spectral intensities of a fully folded state and a fully unfolded state, respectively, and I is an intensity of a spectrum at a given temperature and pressure. I_F and I_U are assumed to be a linear function of temperature or pressure. To determine the value of f, we used the second-derivative IR peak

dx.doi.org/10.1021/bi2019223 | *Biochemistry* 2012, 51, 3539−3546

intensities for natural Cro and SN4m, and the mean residue ellipticity at 222 nm for natural Cro.

The free energy change (ΔG), the enthalpy change (ΔH), and the volume change (ΔV) upon unfolding were obtained using the following equations:

$$-R\left[\frac{\partial \ln K}{\partial(1/T)}\right]_p = \Delta H \quad (3)$$

$$-RT\left(\frac{\partial \ln K}{\partial p}\right)_T = \Delta V \quad (4)$$

RESULTS

Amide I′ Spectra of Natural Cro and SN4m. Figure 2 shows typical infrared spectra of natural Cro and SN4m in the folded state, and their second-derivative spectra at room temperature. The band components that overlapped in the amide I′ region were resolved by the second derivative of the original spectra. The three band components were observed at 1624, 1650, and 1676 cm^{-1} in the second-derivative spectrum of natural Cro. The band at 1650 cm^{-1} typically originates from an α-helical structure.[19−21] The two bands at 1624 and 1676 cm^{-1} originate from the band splitting by the vibrational couplings of the oscillators in the amide groups belonging to the antiparallel β-sheets.[22−24] These structural assignments are consistent with the X-ray crystallographic analysis that identified natural Cro as an $\alpha + \beta$ protein.[11] With respect to SN4m, the second-derivative spectrum reveals three band components at 1629, 1646, and 1676 cm^{-1} and is therefore similar to that of natural Cro. The peak frequency of 1646 cm^{-1} of SN4m is slightly lower than the peak frequency of 1650 cm^{-1} arising from the α-helices in natural Cro. On the basis of previous research, this lower-frequency shift suggests hydration of the carbonyls of the peptide backbone of the α-helices. For example, the hydrated helices of calmodulin and troponin C were assigned to ~1644 cm^{-1},[25] and the highly hydrated α-helix of an alanine-based peptide was assigned to ~1633 cm^{-1}.[26] These observations support the concept that more highly hydrated environments around helices induce lower-frequency shifts. The two bands at 1629 and 1676 cm^{-1} in the spectrum of SN4m were assigned to an antiparallel β-sheet structure. The peak frequency of 1629 cm^{-1} is higher by 5 cm^{-1} than the corresponding band observed for natural Cro, which is probably due to the weakening of hydrogen bonds between β-strands.[27] The band component at 1676 cm^{-1} of natural Cro and SN4m overlaps with a band arising from the asymmetric carboxylate stretching mode of residual TFA ion traces that are present after dialysis.[16] This finding is confirmed by the observation that the band arising from TFA remained above 90

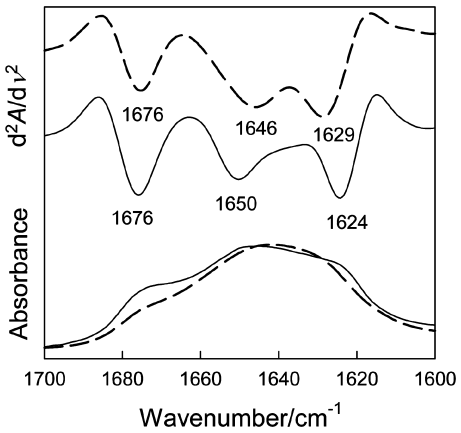

Figure 2. Infrared spectra of the amide I′ region of natural Cro (—) and SN4m (– – –). The second-derivative spectra are also shown.

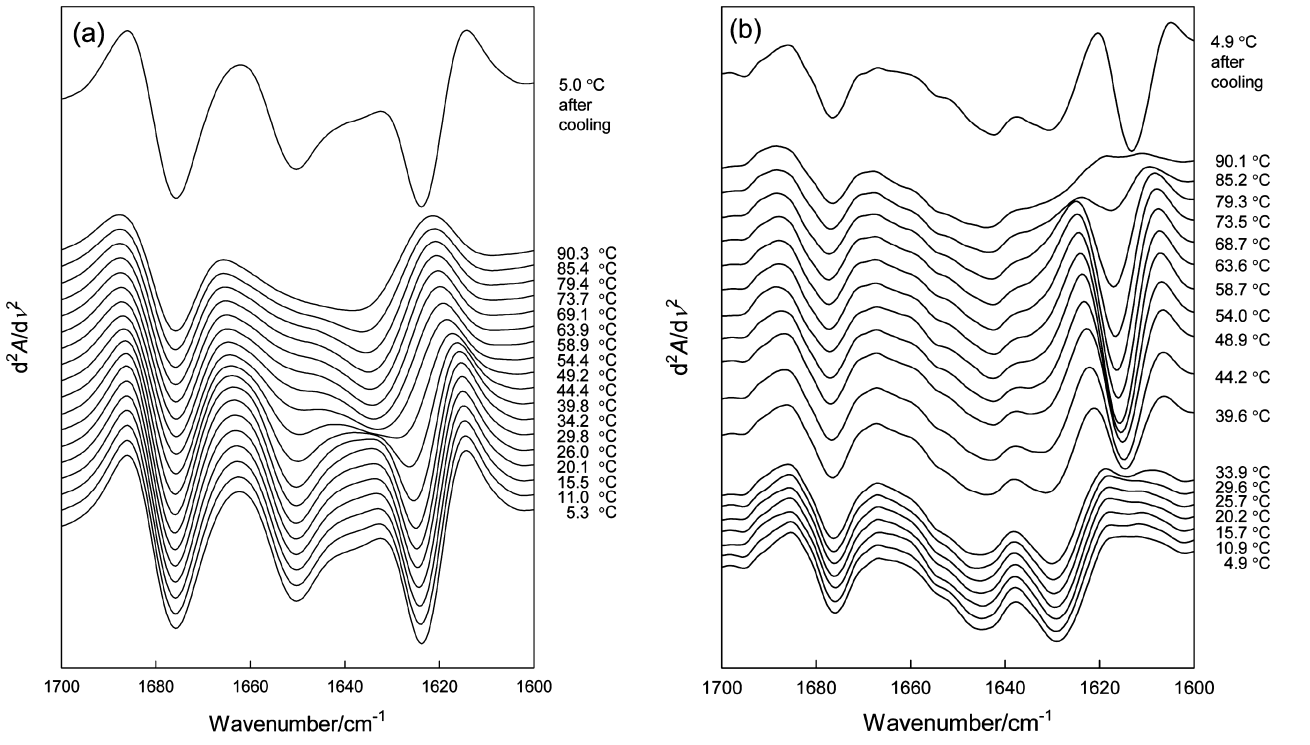

Figure 3. Second-derivative infrared spectra of the amide I′ region of (a) natural Cro and (b) SN4m at various temperatures.

dx.doi.org/10.1021/bi2019223 | *Biochemistry* 2012, 51, 3539−3546

°C, whereas the bands at 1624 cm^{-1} (natural Cro) and 1629 cm^{-1} (SN4m) had disappeared (see below).

Thermal Unfolding of Natural Cro and SN4m. Figure 3 shows the temperature dependence of the second-derivative spectra of the amide I′ absorption of natural Cro and SN4m. In the spectra of natural Cro, the intensities of the bands at 1624, 1650, and 1676 cm^{-1} decrease with an increase in temperature, indicating that the α-helices and the antiparallel β-sheets unfold with an increase in temperature. The spectrum measured after the sample had been cooled from 90.3 to 5.3 °C is almost identical to the spectrum measured at 5.3 °C before thermal unfolding, indicating that the melting transition is reversible. In the spectra of SN4m, the intensities of the bands at 1629 and 1676 cm^{-1} drastically decreased in the temperature range between 25.7 and 63.6 °C, indicating the unfolding of the antiparallel β-sheets. Simultaneously, a new peak at 1616 cm^{-1} appeared at 39.6 °C and increased in intensity until the temperature reached ~54.0 °C. An increase in the peak intensity at 1616 cm^{-1} is indicative of an increase in the level of intermolecular β-sheet structures because of heat-induced aggregation. This behavior is similar to the heat-induced denaturation and aggregation of proteins reported in previous studies.[25,27,28] Interestingly, the intensity of the band at 1616 cm^{-1} decreased with an increase in temperature above 54.0 °C, suggesting the melting of the intermolecular β-sheet structures. The spectrum measured after the sample had been cooled from 90.1 to 4.9 °C shows the peak at 1616 cm^{-1} with significant intensity, indicating the re-formation of the intermolecular β-sheet structures during cooling. White precipitate in the cuvette was visible after the measurement. At the highest temperatures, there is a slight difference in the shape of the spectra between natural Cro and SN4m, indicating that the two proteins show different unfolding behaviors. CD spectroscopic measurements (Figure S1 of the Supporting Information) showed that the ellipticity at 222 nm of natural Cro was ~5000 deg cm^2 $dmol^{-1}$ at 95.7 °C, whereas that of SN4m was ~9000 deg cm^2 $dmol^{-1}$ at 96.5 °C, indicating that heat-induced unfolded SN4m contains residual helix structure.

To examine the thermal unfolding of the secondary structures of natural Cro, we plotted the fractions of the folded α-helices and β-sheets, which are determined from the changes in the second-derivative intensities at 1650 and 1624 cm^{-1}, respectively, according to eq 2, as a function of temperature (Figure 4). The thermal unfolding curves of the α-helices and β-sheets of natural Cro are almost identical to each other, indicating that the secondary structures unfold cooperatively. The temperature dependence of the ellipticity at 222 nm of natural Cro was also examined by CD spectroscopy under the same sample conditions that were used for the IR measurements. The thermal unfolding curve of the α-helices determined from the CD measurement, which is also shown in Figure 4, is also very similar to that determined from the IR analysis, supporting the validity of this IR analysis. From the van't Hoff plots obtained using these multiple probes, we determined the enthalpy changes (ΔH) and the transition temperatures (T_m), as summarized in Table 1. The calculated values are similar to each other. As noted above, the analyses for SN4m were not performed because of the irreversibility of the thermal unfolding above 33.9 °C.

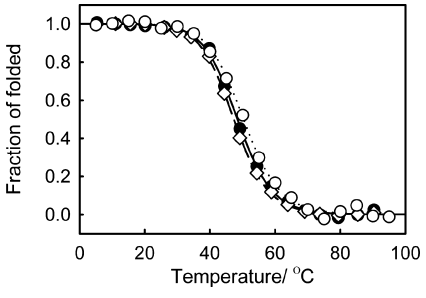

Figure 4. Thermal unfolding curves of natural Cro that were determined from the second-derivative intensity at 1650 cm^{-1} due to the α-helices (filled circles and solid line), the intensity at 1624 cm^{-1} due to the β-sheets (empty diamonds and dashed line), and the CD ellipticity values at 222 nm (empty circles and dotted line). The curves were generated by using the two-state model. The fractions of folded protein were estimated according to eq 1.

Pressure-Induced Unfolding of Natural Cro and SN4m. Figure 5 shows the pressure dependence of the second-derivative spectra of natural Cro and SN4m. In the spectra of natural Cro, the intensities of the bands at 1624, 1650, and 1676 cm^{-1} decreased with an increase in pressure, and the spectra do not significantly change above 716 MPa. The spectrum measured after decompression from 1360 to 0.1 MPa was almost identical to the initial spectrum measured at 0.1 MPa. These spectral changes show a reversible pressure-induced unfolding reaction of the α-helices and the antiparallel β-sheets of natural Cro. In the spectra of SN4m, the intensity of the band at 1629 cm^{-1} due to the β-sheet decreased when the pressure was increased to 462 MPa. The intensity of the band at 1646 cm^{-1} due to the α-helices decreased with an increase in pressure but could still be observed at 646 MPa. This band was absent above 1090 MPa, indicating that most of the α-helices have fully unfolded. The spectrum measured after decompression was almost identical to the spectrum measured at 0.1 MPa. Thus, the transition is reversible. The shapes of the spectra of natural Cro and SN4m at the highest pressure are nearly identical, indicating that the extent of unfolding between these two proteins was comparable. In Figure 6, the fractions of the folded α-helices and β-sheets in natural Cro and SN4m estimated from the changes in the second-derivative intensities are plotted as a function of pressure. The pressure unfolding curves of the α-helices and β-sheets of natural Cro show a sigmoidal shape and are somewhat different from each other. In contrast, there is a marked difference in the pressure unfolding curves between the α-helices and β-sheets of SN4m. The α-helices gradually unfold over the pressure range from 0.1 to ~1000 MPa, whereas the β-sheets steeply unfold over the pressure range from 0.1 to ~400 MPa. This reveals that the cooperativity in the pressure-induced unfolding process of SN4m does not hold. The volume changes upon unfolding (ΔV) and the transition pressures (P_m) of natural Cro and SN4m are summarized in Table 1. The values of ΔV and P_m of natural Cro determined from the unfolding curves of the α-helices and β-sheets are very similar to each other; however, this is not the case for the data recorded for SN4m.

DISCUSSION

This study examined the effects of temperature and pressure on the structure of natural Cro and SN4m. The thermal unfolding of natural Cro is highly cooperative and reversible. The pressure unfolding of natural Cro also appears to be roughly cooperative. Conversely, the thermal unfolding of SN4m is irreversible, and the pressure-induced unfolding is clearly not cooperative. As shown in Figure 6b, the pressure unfolding of

dx.doi.org/10.1021/bi2019223 | Biochemistry 2012, 51, 3539–3546

Table 1. Thermodynamic Parameters of Natural Cro and SN4m upon Unfolding

	ΔH (kJ/mol)	T_m (°C)	ΔV (cm^3/mol)	P_m (MPa)	spectroscopic probe
natural Cro	149 ± 6	48 ± 0.6	−23 ± 1	466 ± 12	IR (1650 cm^{-1})
	160 ± 3	47 ± 0.3	−33 ± 4	362 ± 30	IR (1624 cm^{-1})
	157 ± 1	50 ± 0.03			CD (222 nm)
SN4m	ND	ND	−17 ± 1	618 ± 20	IR (1656 cm^{-1})
			−49 ± 8	253 ± 23	IR (1629 cm^{-1})

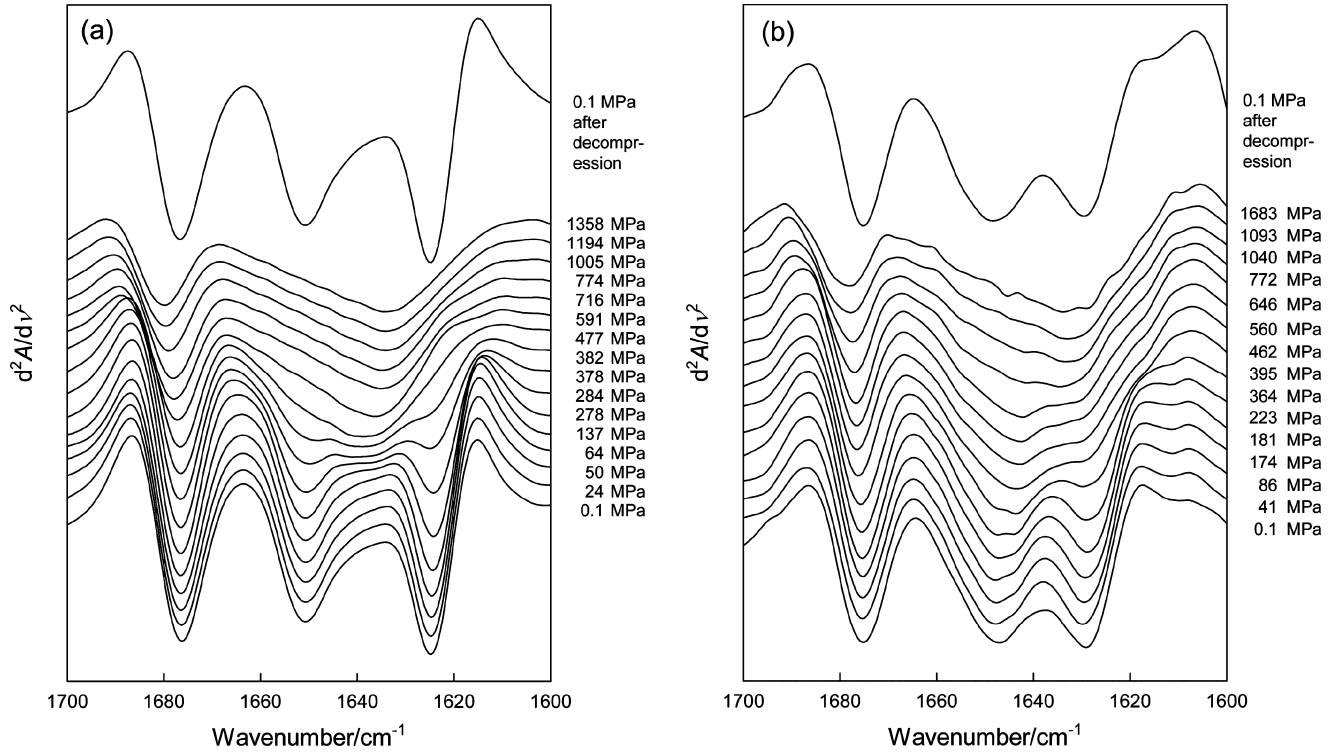

Figure 5. Second-derivative infrared spectra of the amide I′ region of (a) natural Cro and (b) SN4m at various pressures.

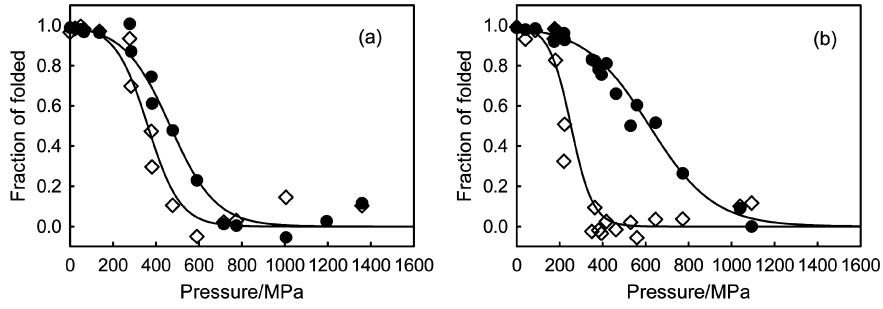

Figure 6. (a) Pressure unfolding curves of natural Cro that were determined from the second-derivative intensities at 1650 cm^{-1} due to the α-helices (●) and the intensity at 1624 cm^{-1} due to the β-sheets (◇). (b) Pressure unfolding curves of SN4m, which were determined from the second-derivative intensities at 1646 cm^{-1} derived from the α-helices (●) and the intensity at 1629 cm^{-1} derived from the β-sheets (◇). The curves were generated using the two-state model. The fractions of folded protein were estimated according to eq 1.

the β-sheets of SN4m is complete at ~400 MPa, whereas most of the α-helices remain intact at this pressure. This implies that the isostatic intermediate state, in which the α-helices are folded and the β-sheets are unfolded, is populated under a pressure of ~400 MPa. The loss of cooperativity of unfolding between the α-helices and β-sheets of SN4m suggests that the interaction between the α-helices and β-sheets is weak and that the stabilities of the α-helices and β-sheets are independent of each other. In previous studies,[5−8] we have demonstrated that α-helices of designed peptides are folded by exerting pressure. These observations are apparently opposed to the generally observed pressure-induced unfolding of natural proteins. To unravel this paradox, we proposed the following model:[7,8] the helices in proteins are significantly stabilized by hydrophobic interactions present in the protein core. In this model, if the loss of the stabilized energy accompanying the pressure-induced destruction of tertiary structure is significantly larger than the stabilization energy ($-p\Delta V$) for helix formation, the helices of proteins unfold under high pressure. This model assumes that a change in the partial molar volume for the helix

dx.doi.org/10.1021/bi2019223 | Biochemistry 2012, 51, 3539−3546

to coil transformation is intrinsically positive. This pressure-induced unfolding of the α-helices of natural Cro can also be explained by this model. Loss of the tertiary contacts between the α-helices and β-sheets with pressure significantly destabilizes the α-helices. On the other hand, the α-helices of SN4m do not unfold under ∼400 MPa, at which pressure the β-sheets have almost completely unfolded. This means that the interaction with β-sheets in SN4m does not significantly contribute to the stabilization of the α-helices. It is noted that peptides of >12 residues are generally required to form a stably folded α-helix.[29] Because the peptide of each α-helix in SN4m has fewer than nine residues, it is likely that the helix−helix interaction is a significant factor in stabilizing the α-helices. Indeed, the helical content prediction for the helical parts of both proteins by the AGADIR algorithm[30−34] gives the following values: 5% for helix 1 (LKDYAMRF), 1% for helix 2 (QTKTAKDL), and 2% for helix 3 (QSAINKAIHA) of natural Cro and 4% for helix 1 (LKKFVE), 7% for helix 2 (QEYAARA), and 50% for helix 3 (QKLIEEVLKR) of SN4m. The helical propensities of the sequences, except that of helix 3 of SN4m, are very low. The high score for helix 3 of SN4m may be related to the residual helical structure in the thermally unfolded state as noted in Results. The low overall values support the assumption described above that the tertiary contacts are important factors for stabilizing the helices. Thus, the unfolding of the α-helices in SN4m at pressures above 400 MPa would result from the pressure-induced destruction of the helix−helix interactions.

As mentioned above, unfolding of the β-sheets of the proteins preceded that of the α-helices in this study, which is not the case for an ideal two-state transition. We also applied a three-state analysis to obtain the volume changes upon unfolding ($\Delta V^{\text{three-state}}$). If the α-helices start to unfold after the β-sheets completely unfold, the fraction of the folded β-sheets and the fraction of the unfolded α-helices correspond to the fraction of the folded state, $f_F^{\text{three-state}}$, and unfolded state, $f_U^{\text{three-state}}$, respectively. From the unfolding curves of the α-helices and β-sheets shown in Figure 6, we estimated the fraction of $f_F^{\text{three-state}}$ and $f_U^{\text{three-state}}$ and calculated the $\Delta V^{\text{three-state}}$ to be −32 cm^3/mol for natural Cro and −40 cm^3/mol for SN4m. Although a relationship between the three-dimensional structure of a protein and the ΔV is still an outstanding issue,[1,4] e.g., the volume change upon hydration of the hydrophobic residues located at the protein interior in the folded state is an ambiguous factor, it has been hypothesized and well accepted that the loss of the solvent inaccessible voids contributes largely to the negative change in volume upon unfolding of proteins.[2,35] On the basis of this hypothesis, the magnitude of ΔV of SN4m is expected to be smaller because the folded structure of SN4m is loosely packed, which probably reduces the size of the solvent inaccessible voids, as indicated by the IR band of the hydrated helices. However, the magnitude of ΔV of SN4m is comparable or slightly larger than that of natural Cro. A possible explanation is that the imperfect packing in the core residues of SN4m may make the void volume larger.

Investigating factors that have caused the loss of folding cooperativity of SN4m is worthwhile for the future redesign of proteins. In a previous study,[11] Phe63 in natural Cro was found to be an essential core residue for its folding, which is packed into the boundary between the α-helices and β-sheets. The corresponding residue, Phe63, in the NMR structure of SN4m is directed toward the exterior of the core.[15] Nevertheless, SN4m has been characterized as being stably folded into a single structure; its free energy difference between the unfolded and folded states (ΔG = −2.5 kcal/mol; the value is estimated by assuming the two-state model)[15] is comparable to that of natural Cro (ΔG = −3 kcal/mol).[36] This observation indicates that SN4m is not essentially stabilized by Phe63. The loss of stability may be compensated by the helix−helix interactions, as suggested by the stronger pressure resistance of the helices of SN4m. An increase in the stability of the helices through the interactions within the helical regions may result in the loss of cooperativity. In studies of ribonuclease A,[37,38] the substitution of Val for Phe46, which exists in the hydrophobic core, resulted in an increase in the cavity volume and a loss of folding cooperativity. The authors suggested that Phe46 (the wild-type residue) contributes to the highly packed core and connects two structural domains, which produces the high folding cooperativity.[37,38] Similarly, this case suggests that significant packing around Phe63 in the core would represent important factors that facilitate folding cooperativity. In addition, the numbers of side chain−side chain hydrogen bonds, which were determined to be 10 for natural Cro and two for SN4m using Discovery Studio Visualizer version 2.5.5 (Accelrys Software Inc., San Diego, CA), are also important. Thus, the richness of the hydrogen bonds between side chains and the tight packing in the core region of natural Cro may contribute to the maintenance of the tertiary contacts and facilitation of the higher folding cooperativity.

We observed that SN4m undergoes heat-induced aggregation whereas natural Cro does not. An unfolded polypeptide containing a large number of hydrophobic amino acid residues often forms intermolecular aggregations, especially at higher temperatures. The hydrophobicity of SN4m, which was calculated using the classical method developed by Kyte and Doolittle,[39] is comparable to that of natural Cro (Figure S2 of the Supporting Information). In addition, it is interesting that the intermolecular β-sheets melt at higher temperatures, at which SN4m unfolds. The instability of the intermolecular assembly of proteins at higher temperatures has been observed in other studies.[40,41] In the past decade, it has been widely accepted that partially unfolded states of proteins are susceptible to aggregation.[42−44] Partially unfolded SN4m, which exposes the internal hydrophobic side chains to water and gives rise to an increase in the number of nonspecific intermolecular contacts via hydrophobic interactions, is a likely a source of the insoluble aggregates.

Figure 7 illustrates the folding free energy landscapes for natural Cro and SN4m. There are two main minima of the folded and unfolded states of natural Cro. On the other hand, in the case of SN4m, the partially folded intermediate state is able to be populated at moderate pressures (∼400 MPa). These findings are consistent with the hypothesis that the sequences of naturally occurring proteins have evolved to destabilize their intermediates.[45−49] The sequence of SN4m is not explicitly exposed to any evolutionary pressure. Conversely, the sequence of natural Cro is optimized by evolutionary pressure to destabilize the intermediate state(s), which is accomplished by stabilizing their secondary structures interdependently. Additionally, the heat-induced aggregation of SN4m implies that the destabilization of folding intermediates for avoiding the formation of irreversible intermolecular aggregation is a major driving force in the natural selection of protein sequences.

In summary, this study has shown that the α-helices and β-sheets of natural Cro cooperatively and reversibly unfold under

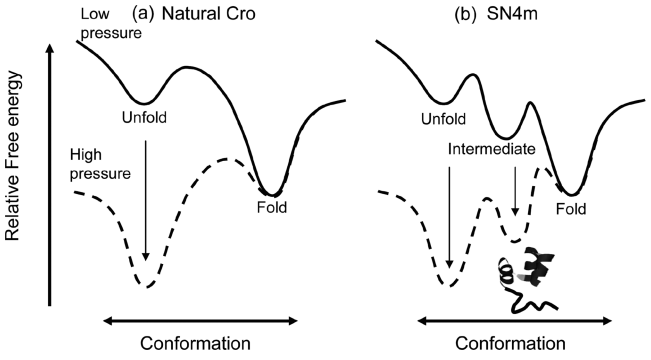

Figure 7. Schematic illustration showing the effect of pressure on the folding free energy landscape of (a) natural Cro and (b) SN4m.

temperature- and pressure-induced denaturation, whereas the secondary structure elements of SN4m are irreversibly unfolded by temperature and do not cooperatively unfold under pressure-induced denaturation. The stabilities of the secondary structure elements of natural Cro are dependent on each other, whereas those of SN4m are stabilized independently. The α-helices in the folded state of SN4m are stabilized by local tertiary contacts among the α-helices, rather than global tertiary contacts between the α-helices and β-sheets. In a previous study, we proposed that α-helices are intrinsically not unfolded by pressure. The pressure-induced unfolding of α-helices described here results from pressure-induced destruction of tertiary contacts that are indispensable for the stabilization of the α-helices. This study also demonstrated that the use of pressure aids the identification of interactions that govern the folding cooperativity of proteins, including artificially designed proteins.

■ ASSOCIATED CONTENT

Ⓢ Supporting Information

CD spectra of natural Cro and SN4m and hydrophobicities calculated by the Kyte−Doolittle method. This material is available free of charge via the Internet at http://pubs.acs.org.

■ AUTHOR INFORMATION

Corresponding Author

*E-mail: kato-m@ph.ritsumei.ac.jp. Phone: +81-77-561-2761. Fax: +81-77-561-2659.

Funding

This study was supported in part by grants-in-aid for Scientific Research from the Ministry of Education, Culture, Sports, Science, and Technology of Japan.

Notes

The authors declare no competing financial interest.

■ ACKNOWLEDGMENTS

We thank Prof. Ryo Kitahara (Ritsumeikan University) and Prof. Motonori Ota (Nagoya University, Nagoya, Japan) for fruitful discussions.

■ ABBREVIATIONS

FTIR, Fourier transform infrared; NMR, nuclear magnetic resonance; CD, circular dichroism; PDB, Protein Data Bank.

■ REFERENCES

(1) Chalikian, T. V., and Breslauer, K. J. (1998) On the volume changes accompanying conformational transitions of biopolymers. *Biopolymers 39*, 619−626.
(2) Frye, K. J., and Royer, C. A. (1998) Probing the contribution of internal cavities to the volume change of protein unfolding under pressure. *Protein Sci. 7*, 2217−2222.
(3) Chalikian, T. V. (2003) Volumetric properties of proteins. *Annu. Rev. Biophys. Biomol. Struct. 32*, 207−235.
(4) Chalikian, T. V., and Macgregor, R. B., Jr. (2009) Origins of pressure-induced protein transitions. *J. Mol. Biol. 394*, 834−842.
(5) Takekiyo, T., Shimizu, A., Kato, M., and Taniguchi, Y. (2005) Pressure-tuning FT-IR spectroscopic study on the helix-coil transition of Ala-rich oligopeptide in aqueous solution. *Biochim. Biophys. Acta 1750*, 1−4.
(6) Takekiyo, T., Takeda, N., Isogai, Y., Kato, M., and Taniguchi, Y. (2007) Pressure stability of the α-helix structure in a de novo designed protein $(\alpha\text{-l-}\alpha)_2$ studied by FTIR spectroscopy. *Biopolymers 85*, 185−188.
(7) Imamura, H., and Kato, M. (2009) Effect of pressure on helix-coil transition of an alanine-based peptide: An FTIR study. *Proteins 75*, 911−918.
(8) Imamura, H., Isogai, Y., Takekiyo, T., and Kato, M. (2010) Effect of pressure on the secondary structure of coiled coil peptide GCN4-p1. *Biochim. Biophys. Acta 1804*, 193−198.
(9) Meersman, F., Smeller, L., and Heremans, K. (2002) Comparative Fourier transform infrared spectroscopy study of cold-, pressure-, and heat-induced unfolding and aggregation of myoglobin. *Biophys. J. 82*, 2635−2644.
(10) Takeda, N., Kato, M., and Taniguchi, Y. (1995) Pressure- and thermally-induced reversible changes in the secondary structure of ribonuclease A studied by FT-IR spectroscopy. *Biochemistry 34*, 5980−5987.
(11) Mossing, M. C., and Sauer, R. T. (1990) Stable, monomeric variants of λ Cro obtained by insertion of a designed β-hairpin sequence. *Science 250*, 1712−1715.
(12) Panick, G., and Winter, R. (2000) Pressure-induced unfolding/refolding of ribonuclease A: Static and kinetic Fourier transform infrared spectroscopy study. *Biochemistry 39*, 1862−1869.
(13) Smeller, L., Meersman, F., and Heremans, K. (2006) Refolding studies using pressure: The folding landscape of lysozyme in the pressure-temperature plane. *Biochim. Biophys. Acta 1764*, 497−505.
(14) Herberhold, H., and Winter, R. (2002) Temperature- and pressure-induced unfolding and refolding of ubiquitin: A static and kinetic Fourier transform infrared spectroscopy study. *Biochemistry 41*, 2396−2401.
(15) Isogai, Y., Ito, Y., Ikeya, T., Shiro, Y., and Ota, M. (2005) Design of λ Cro fold: Solution structure of a monomeric variant of the de novo protein. *J. Mol. Biol. 354*, 801−814.
(16) Andrushchenko, V. V., Vogel, H. J., and Prenner, E. J. (2007) Optimization of the hydrochloric acid concentration used for trifluoroacetate removal from synthetic peptides. *J. Pept. Sci. 13*, 37−43.
(17) Creighton, T. E. (1993) *Proteins, Structures and Molecular Properties*. 2nd ed., Freeman, New York.
(18) Wong, P. T. T., Moffatt, D. J., and Baudais, F. L. (1985) Crystalline quartz as an internal pressure calibrant for high-pressure infrared spectroscopy. *Appl. Spectrosc. 39*, 733−735.
(19) Krimm, S., and Bandekar, J. (1986) Vibrational spectroscopy and conformation of peptides, polypeptides, and proteins. *Adv. Protein Chem. 38*, 181−364.
(20) Surewicz, W. K., Mantsch, H. H., and Chapman, D. (1993) Determination of protein secondary structure by Fourier transform infrared spectroscopy: A critical assessment. *Biochemistry 32*, 389−394.
(21) Barth, A., and Zscherp, C. (2002) What vibrations tell us about proteins. *Q. Rev. Biophys. 35*, 369−430.
(22) Krimm, S., and Abe, Y. (1972) Intermolecular interaction effects in the amide I vibrations of polypeptides. *Proc. Natl. Acad. Sci. U.S.A. 69*, 2788−2792.

(23) Moore, W. H., and Krimm, S. (1975) Transition dipole coupling in Amide I modes of β-polypeptides. *Proc. Natl. Acad. Sci. U.S.A. 72*, 4933−4935.
(24) Torii, H., and Tasumi, M. (1992) Model calculations on the amide-I infrared bands of globular proteins. *J. Chem. Phys. 96*, 3379−3387.
(25) Jackson, M., Haris, P. I., and Chapman, D. (1991) Fourier transform infrared spectroscopic studies of Ca^{2+}-binding proteins. *Biochemistry 30*, 9681−9686.
(26) Martinez, G., and Millhauser, G. (1995) FTIR spectroscopy of alanine-based peptides: Assignment of the amide I′ modes for random coil and helix. *J. Struct. Biol. 114*, 23−27.
(27) Jackson, M., and Mantsch, H. H. (1995) The use and misuse of FTIR spectroscopy in the determination of protein structure. *Crit. Rev. Biochem. Mol. Biol. 30*, 95−120.
(28) Okuno, A., Kato, M., and Taniguchi, Y. (2006) The secondary structure of pressure- and temperature-induced aggregates of equine serum albumin studied by FT-IR spectroscopy. *Biochim. Biophys. Acta 1764*, 1407−1412.
(29) Luo, P., and Baldwin, R. L. (1997) Mechanism of helix induction by trifluoroethanol: A framework for extrapolating the helix-forming properties of peptides from trifluoroethanol/water mixtures back to water. *Biochemistry 36*, 8413−8421.
(30) Munoz, V., and Serrano, L. (1994) Elucidating the folding problem of helical peptides using empirical parameters. *Nat. Struct. Biol. 1*, 399−409.
(31) Munoz, V., and Serrano, L. (1995) Elucidating the folding problem of helical peptides using empirical parameters. II. Helix macrodipole effects and rational modification of the helical content of natural peptides. *J. Mol. Biol. 245*, 275−296.
(32) Munoz, V., and Serrano, L. (1995) Elucidating the folding problem of helical peptides using empirical parameters. III. Temperature and pH dependence. *J. Mol. Biol. 245*, 297−308.
(33) Munoz, V., and Serrano, L. (1997) Development of the multiple sequence approximation within the AGADIR model of α-helix formation: Comparison with Zimm-Bragg and Lifson-Roig formalisms. *Biopolymers 41*, 495−509.
(34) Lacroix, E., Viguera, A. R., and Serrano, L. (1998) Elucidating the folding problem of α-helices: Local motifs, long-range electrostatics, ionic-strength dependence and prediction of NMR parameters. *J. Mol. Biol. 284*, 173−191.
(35) Royer, C. A. (2002) Revisiting volume changes in pressure induced protein unfolding. *Biochim. Biophys. Acta 1595*, 201−209.
(36) Jana, R., Hazbun, T. R., Mollah, A. K., and Mossing, M. C. (1997) A folded monomeric intermediate in the formation of λ Cro dimer-DNA complexes. *J. Mol. Biol. 273*, 402−416.
(37) Chatani, E., Nonomura, K., Hayashi, R., Balny, C., and Lange, R. (2002) Comparison of heat- and pressure-induced unfolding of ribonuclease A: The critical role of Phe46 which appears to belong to a new hydrophobic chain-folding initiation site. *Biochemistry 41*, 4567−4574.
(38) Kadonosono, T., Chatani, E., Hayashi, R., Moriyama, H., and Ueki, T. (2003) Minimization of cavity size ensures protein stability and folding: Structures of Phe46-replaced bovine pancreatic RNase A. *Biochemistry 42*, 10651−10658.
(39) Kyte, J., and Doolittle, R. F. (1982) A simple method for displaying the hydropathic character of a protein. *J. Mol. Biol. 157*, 105−132.
(40) Morel, B., Varela, L., and Conejero-Lara, F. (2010) The thermodynamic stability of amyloid fibrils studied by differential scanning calorimetry. *J. Phys. Chem. B 114*, 4010−4019.
(41) Kardos, J., Micsonai, A., Pal-Gabor, H., Petrik, E., Graf, L., Kovacs, J., Lee, Y. H., Naiki, H., and Goto, Y. (2011) Reversible heat-induced dissociation of β2-microglobulin amyloid fibrils. *Biochemistry 50*, 3211−3220.
(42) Booth, D. R., Sunde, M., Bellotti, V., Robinson, C. V., Hutchinson, W. L., Fraser, P. E., Hawkins, P. N., Dobson, C. M., Radford, S. E., Blake, C. C., and Pepys, M. B. (1997) Instability, unfolding and aggregation of human lysozyme variants underlying amyloid fibrillogenesis. *Nature 385*, 787−793.
(43) Dobson, C. M. (2003) Protein folding and misfolding. *Nature 426*, 884−890.
(44) Jahn, T. R., and Radford, S. E. (2005) The Yin and Yang of protein folding. *FEBS J. 272*, 5962−5970.
(45) Isogai, Y. (2006) Native protein sequences are designed to destabilize folding intermediates. *Biochemistry 45*, 2488−2492.
(46) Brockwell, D. J., and Radford, S. E. (2007) Intermediates: Ubiquitous species on folding energy landscapes? *Curr. Opin. Struct. Biol. 17*, 30−37.
(47) Watters, A. L., Deka, P., Corrent, C., Callender, D., Varani, G., Sosnick, T., and Baker, D. (2007) The highly cooperative folding of small naturally occurring proteins is likely the result of natural selection. *Cell 128*, 613−624.
(48) Honda, S., Akiba, T., Kato, Y. S., Sawada, Y., Sekijima, M., Ishimura, M., Ooishi, A., Watanabe, H., Odahara, T., and Harata, K. (2008) Crystal structure of a ten-amino acid protein. *J. Am. Chem. Soc. 130*, 15327−15331.
(49) Isogai, Y., Ishii, A., Fujisawa, T., Ota, M., and Nishikawa, K. (2000) Redesign of artificial globins: Effects of residue replacements at hydrophobic sites on the structural properties. *Biochemistry 39*, 5683−5690.